Flexural-torsional behavior of thin-walled composite space frames

Thuc Phuong Vo* and Jaehong Lee†

Department of Architectural Engineering, Sejong University
98 Kunja Dong, Kwangjin Ku, Seoul 143-747, Korea

(Dated: September 14, 2009)

A general analytical model based on the first-order shear deformable beam theory applicable to thin-walled composite space frames with arbitrary lay-ups under external loads is presented. This model accounts for all the structural coupling coming from the material anisotropy. The seven governing equations are derived from the principle of the stationary value of total potential energy. A displacement-based one-dimensional 14 degree-of-freedom space beam model which includes the effects of shear deformation, warping is developed to solve the problem. Numerical results are obtained to investigate the effects of fiber orientation on flexural-torsional responses of thin-walled composite space frame under vertical load.

Keywords: thin-walled composite space frames; shear deformation; flexural-torsional responses.

I. INTRODUCTION

Fiber-reinforced composite materials have been used over the past few decades in a variety of structures. Composites have many desirable characteristics, such as high ratio of stiffness and strength to weight, corrosion resistance and magnetic transparency. Thin-walled structural shapes made up of composite materials, which are usually produced by pultrusion, are being increasingly used in many engineering fields.

The analysis of thin-walled structures has received considerable attention by researchers using both the continuum mechanics approach and the finite element approach since the development of the comprehensive theory of torsion and bending of thin-walled bars by Vlasov [1] and Gjelsvik [2]. For thin-walled composite beams, the studies carried out so far may broadly be divided into two groups. The first and most common approach is based on an analytical

*Graduate student

†Professor, corresponding author. Tel.:+82-2-3408-3287; fax:+82-2-3408-3331

; Electronic address: jhlee@sejong.ac.kr

technique, while the other approach requires a two-dimensional finite element analysis to obtain the cross-section stiffness matrix. Hodges and co-workers [3-5] pioneered the second approach, which was referred to as the so-called variational asymptotic beam section analysis. It was based on the variational asymptotic method (VAM), where the three dimensional elasticity problem was systematically divided into a two dimensional cross-sectional problem, and a one dimensional beam problem (length direction). It should be mentioned that Hodges and co-workers (e.g., Volovoi et al. [3,4], Yu et al. [5]) further applied the concept introduced by VAM to two dimensional cross-sectional problem and derived closed-form expressions for the cross-sectional stiffness coefficients of thin-walled beams. In the present investigation, an analytical approach is adopted for the derivation of the cross-sectional stiffness matrix considering different effects and their coupling to yield a general formulation. By using this analytical approach, up to the now, the investigation on static and dynamic behavior of thin-walled composite beams has been carried out extensively since the early works of Bauld and Tzeng [6] and Chandra and Chopra [7]. A general beam model for thin-walled open and closed section composite beams which included the effect of shear deformation and restrained warping are found in the monographs [8, 9]. Salim and Davalos [10] presented the linear analysis of open and closed sections made of general laminated composites by extending Gjelsvik's model. This model accounted for all possible elastic couplings in composite sections, such as extension- and bending-torsion. Pluzsik and Kollar [11] introduced a theory for thin-walled, closed section, orthotropic beams which took into account the shear deformation in restrained warping induced torque. Kim et al.[12,13] developed not only exact solutions for general thin-walled open-section composite beams under torsional moment but also the exact stiffness matrix of mono-symmetric composite I-beams with arbitrary lamination. Piovan and Cortinez [14] presented a new theoretical model for the generalized linear analysis of thin-walled beams with open or closed cross-sections. By employing a non-linear displacement field, this model allowed studying many problems of static, free vibrations with or without arbitrary initial stresses and linear stability of composite thin-walled beams with general cross-sections. Back and Will [15] developed a shear-flexible finite element based on an orthogonal Cartesian coordinate system for the flexural and buckling analyzes of thin-walled composite I-beams with both doubly and mono-symmetrical cross-sections. Sheikh and Thomsen [16] introduced a condensed fully coupled beam element for thin-walled laminated composite beams having open or closed cross sections. An analytical technique was used to derive the cross-sectional stiffness of the beam in a systematic manner considering all the deformation effects and their mutual couplings.

Thin-walled space frames are the most common load-carrying systems in engineering application. Thin-walled sections, such as I-section, channel and angle, are appealing because they offer a high performance in terms of

minimum weight for given strength. A literature survey on this subject shows that although a large number of studies performed on the analysis of isotropic thin-walled space frames, only some works dealt with thin-walled composite structures with arbitrary lay-ups. It is due to the fact that these structures are often very thin and have complicated material anisotropy. The widespread application of thin-walled composite frames will require much work in the area of material, manufacturing, fabrication, analysis and design. By extending a one-dimensional beam concept developed in an earlier paper [17] for isotropic thin-walled frames, Noor et al. [18] performed on the free vibrations of thin-walled semicircular graphite-epoxy composite frames. The semicircular thin-walled frames with I- and J-sections were considered in analysis. A mixed formulation was used with the fundamental unknowns consisting of both the generalized displacements and stress resultants in frames. Experiments were conducted by Collins and Johnson [19] to measure the three-dimensional static and vibratory response of two graphite-epoxy thin-walled open section frames including symmetric I-section and an asymmetric channel section. The works of Bank and Cofie [20-24] deserved special attention because they developed a novel method for the analysis of thin-walled composite frames. To account for the effects of warping and anisotropy, the model described by Cofie [20,21] for isotropic beam elements was extended to include anisotropy and used to develop the element stiffness matrix for analyzing thin-walled anisotropic frames. The beam was divided into two regions, a warping region, and a non-warping region. The warping superelement was used in the region of the beam where warping was considered critical. The non-warping element was used outside of this critical region. An open section thin-walled thermoplastic composite frame segment (sub-element) of a mass transit bus was designed, analyzed and manufactured by Ning et al. [25] to replace a conventional metal-based design. Recently, a locking-free finite element formulation for the buckling and vibration analysis of orthotropic fiber-reinforced polymers thin-walled frames with open section was introduced by Minghini et al. [26-28]. A second-order approximation of the displacement field was adopted to account for the shear strain effects on both non-uniform torsion and bending. Besides, joint flexibility at member ends was also included by means of a simple manipulation of the stiffness matrix to the finite element, such that the influence of joint behavior on membrane, shear, bending and torsion deformations, as well as cross-section warping was taken into account.

In this paper, which is an extension of the authors' previous works [29-31], flexural-torsional analysis of thin-walled composite space frames with arbitrary lay-ups under external loads is presented. This model is based on the first-order shear deformable beam theory, and accounts for all the structural coupling coming from the material anisotropy. The seven governing equations are derived from the principle of the stationary value of total potential energy. Numerical results are obtained for thin-walled composite space frame under vertical load to investigate effects of fiber angle on

flexural-torsional responses.

II. KINEMATICS

The theoretical developments presented in this paper require two sets of coordinate systems which are mutually interrelated. The first coordinate system is the orthogonal Cartesian coordinate system (x, y, z), for which the x- and y-axes lie in the plane of the cross section and the z axis parallel to the longitudinal axis of the beam. The second coordinate system is the local plate coordinate (n, s, z) as shown in Fig. 1, wherein the n axis is normal to the middle surface of a plate element, the s axis is tangent to the middle surface and is directed along the contour line of the cross section. The (n, s, z) and (x, y, z) coordinate systems are related through an angle of orientation θ. As defined in Fig.1 a point P, called the pole, is placed at an arbitrary point x_p, y_p. A line through P parallel to the z axis is called the pole axis.

To derive the analytical model for thin-walled composite beams, the following assumptions are made:

1. The contour of the thin wall does not deform in its own plane.

2. Transverse shear strains $\gamma^{\circ}_{xz}, \gamma^{\circ}_{yz}$ and warping shear γ°_{ω} are incorporated. It is assumed that they are uniform over the cross-sections.

According to assumption 1, the midsurface displacement components $\bar{u}, \bar{v}$ at a point A in the contour coordinate system can be expressed in terms of a displacements U, V of the pole P in the x, y directions, respectively, and the rotation angle Φ about the pole axis,

$$\bar{u}(s, z) = U(z) \sin\theta(s) - V(z) \cos\theta(s) - \Phi(z) q(s) \tag{1a}$$

$$\bar{v}(s, z) = U(z) \cos\theta(s) + V(z) \sin\theta(s) + \Phi(z) r(s) \tag{1b}$$

These equations apply to the whole contour. The out-of-plane shell displacement $\bar{w}$ can now be found from the assumption 2. For each element of middle surface, the midsurface shear strains in the contour can be expressed with respect to the transverse shear and warping shear strains.

$$\bar{\gamma}_{nz}(s, z) = \gamma^{\circ}_{xz}(z) \sin\theta(s) - \gamma^{\circ}_{yz}(z) \cos\theta(s) - \gamma^{\circ}_{\omega}(z) q(s) \tag{2a}$$

$$\bar{\gamma}_{sz}(s, z) = \gamma^{\circ}_{xz}(z) \cos\theta(s) + \gamma^{\circ}_{yz}(z) \sin\theta(s) + \gamma^{\circ}_{\omega}(z) r(s) \tag{2b}$$

Further, it is assumed that midsurface shear strain in $s - n$ direction is zero ($\bar{\gamma}_{sn} = 0$). From the definition of the

shear strain, $\bar{\gamma}_{sz} = 0$ can also be given for each element of middle surface as:

$$\bar{\gamma}_{sz}(s,z) = \frac{\partial \bar{v}}{\partial z} + \frac{\partial \bar{w}}{\partial s} \tag{3}$$

After substituting for $\bar{v}$ from Eq.(1) into Eq.(3) and considering the following geometric relations,

$$dx = ds\cos\theta \tag{4a}$$

$$dy = ds\sin\theta \tag{4b}$$

Displacement $\bar{w}$ can be integrated with respect to s from the origin to an arbitrary point on the contour,

$$\bar{w}(s,z) = W(z) + \Psi_y(z)x(s) + \Psi_x(z)y(s) + \Psi_\omega(z)\omega(s) \tag{5}$$

where Ψ_x, Ψ_y and Ψ_ω represent rotations of the cross section with respect to x, y and ω, respectively, given by:

$$\Psi_y = \gamma^\circ_{xz}(z) - U' \tag{6a}$$

$$\Psi_x = \gamma^\circ_{yz}(z) - V' \tag{6b}$$

$$\Psi_\omega = \gamma^\circ_{\omega}(z) - \Phi' \tag{6c}$$

When the transverse shear effect is ignored, Eq.(6) degenerates to $\Psi_y = -U'$, $\Psi_x = -V'$ and $\Psi_\omega = -\Phi'$. As a result, the number of unknown variables reduces to four leading to the Euler-Bernoulli beam model. The prime ($'$) is used to indicate differentiation with respect to z; and ω is the so-called sectorial coordinate or warping function given by

$$\omega(s) = \int_{s_\circ}^{s} r(s)ds \tag{7a}$$

The displacement components u, v, w representing the deformation of any generic point on the profile section are given with respect to the midsurface displacements $\bar{u}, \bar{v}, \bar{w}$ by assuming the first order variation of inplane displacements v, w through the thickness of the contour as:

$$u(s,z,n) = \bar{u}(s,z) \tag{8a}$$

$$v(s,z,n) = \bar{v}(s,z) + n\bar{\psi}_s(s,z) \tag{8b}$$

$$w(s,z,n) = \bar{w}(s,z) + n\bar{\psi}_z(s,z) \tag{8c}$$

where, $\bar{\psi}_s$ and $\bar{\psi}_z$ denote the rotations of a transverse normal about the z and s axis, respectively. These functions can be determined by considering that the midsurface shear strains γ_{nz} is given by definition:

$$\bar{\gamma}_{nz}(s,z) = \frac{\partial \bar{w}}{\partial n} + \frac{\partial \bar{u}}{\partial z} \tag{9}$$

By comparing Eq.(2) and (9), the function can $\bar{\psi}_z$ can be written as

$$\bar{\psi}_z = \Psi_y \sin\theta - \Psi_x \cos\theta - \Psi_\omega q \tag{10}$$

Similarly, using the assumption that the shear strain γ_{sn} should vanish at midsurface, the function $\bar{\psi}_s$ can be obtained

$$\bar{\psi}_s = -\frac{\partial \bar{u}}{\partial s} \tag{11}$$

The strains associated with the small-displacement theory of elasticity are given by

$$\epsilon_s(s,z,n) = \bar{\epsilon}_s(s,z) + n\bar{\kappa}_s(s,z) \tag{12a}$$

$$\epsilon_z(s,z,n) = \bar{\epsilon}_z(s,z) + n\bar{\kappa}_z(s,z) \tag{12b}$$

$$\gamma_{sz}(s,z,n) = \bar{\gamma}_{sz}(s,z) + n\bar{\kappa}_{sz}(s,z) \tag{12c}$$

$$\gamma_{nz}(s,z,n) = \bar{\gamma}_{nz}(s,z) + n\bar{\kappa}_{nz}(s,z) \tag{12d}$$

where

$$\bar{\epsilon}_s = \frac{\partial \bar{v}}{\partial s}; \quad \bar{\epsilon}_z = \frac{\partial \bar{w}}{\partial z} \tag{13a}$$

$$\bar{\kappa}_s = \frac{\partial \bar{\psi}_s}{\partial s}; \quad \bar{\kappa}_z = \frac{\partial \bar{\psi}_z}{\partial z} \tag{13b}$$

$$\bar{\kappa}_{sz} = \frac{\partial \bar{\psi}_z}{\partial s} + \frac{\partial \bar{\psi}_s}{\partial z}; \quad \bar{\kappa}_{nz} = 0 \tag{13c}$$

All the other strains are identically zero. In Eq.(13), $\bar{\epsilon}_s$ and $\bar{\kappa}_s$ are assumed to be zero, and $\bar{\epsilon}_z$, $\bar{\kappa}_z$ and $\bar{\kappa}_{sz}$ are midsurface axial strain and biaxial curvature of the shell, respectively. The above shell strains can be converted to beam strain components by substituting Eqs.(1), (5) and (8) into Eq.(13) as

$$\bar{\epsilon}_z = \epsilon_z^\circ + x\kappa_y + y\kappa_x + \omega\kappa_\omega \tag{14a}$$

$$\bar{\kappa}_z = \kappa_y \sin\theta - \kappa_x \cos\theta - \kappa_\omega q \tag{14b}$$

$$\bar{\kappa}_{sz} = \kappa_{sz} \tag{14c}$$

where $\epsilon_z^\circ, \kappa_x, \kappa_y, \kappa_\omega$ and κ_{sz} are axial strain, biaxial curvatures in the x and y direction, warping curvature with

respect to the shear center, and twisting curvature in the beam, respectively defined as

$$\epsilon_z^\circ = W' \tag{15a}$$

$$\kappa_x = \Psi_x' \tag{15b}$$

$$\kappa_y = \Psi_y' \tag{15c}$$

$$\kappa_\omega = \Psi_\omega' \tag{15d}$$

$$\kappa_{sz} = \Phi' - \Psi_\omega \tag{15e}$$

The resulting strains can be obtained from Eqs.(12) and (14) as

$$\epsilon_z = \epsilon_z^\circ + (x + n\sin\theta)\kappa_y + (y - n\cos\theta)\kappa_x + (\omega - nq)\kappa_\omega \tag{16a}$$

$$\gamma_{sz} = \gamma_{xz}^\circ \cos\theta + \gamma_{yz}^\circ \sin\theta + \gamma_\omega^\circ r + n\kappa_{sz} \tag{16b}$$

$$\gamma_{nz} = \gamma_{xz}^\circ \sin\theta - \gamma_{yz}^\circ \cos\theta - \gamma_\omega^\circ q \tag{16c}$$

III. VARIATIONAL FORMULATION

Total potential energy of the system is calculated by sum of strain energy and the work done by external forces

$$\Pi = \mathcal{U} + \mathcal{V} \tag{17}$$

where $\mathcal{U}$ is the strain energy

$$\mathcal{U} = \frac{1}{2}\int_v (\sigma_z\epsilon_z + \sigma_{sz}\gamma_{sz} + \sigma_{nz}\gamma_{nz})dv \tag{18}$$

The strain energy is calculated by substituting Eq.(16) into Eq.(18)

$$\begin{aligned}\mathcal{U} = \frac{1}{2}\int_v \Big\{ & \sigma_z\Big[\epsilon_z^\circ + (x + n\sin\theta)\kappa_y + (y - n\cos\theta)\kappa_x + (\omega - nq)\kappa_\omega\Big] \\ & + \sigma_{sz}\Big[\gamma_{xz}^\circ\cos\theta + \gamma_{yz}^\circ\sin\theta + \gamma_\omega^\circ r + n\kappa_{sz}\Big] + \sigma_{nz}\Big[\gamma_{xz}^\circ\sin\theta - \gamma_{yz}^\circ\cos\theta - \gamma_\omega^\circ q\Big]\Big\} dv\end{aligned} \tag{19}$$

The variation of the strain energy, Eq.(19), can be stated as

$$\delta\mathcal{U} = \int_0^l (N_z\delta\epsilon_z + M_y\delta\kappa_y + M_x\delta\kappa_x + M_\omega\delta\kappa_\omega + V_x\delta\gamma_{xz}^\circ + V_y\delta\gamma_{yz}^\circ + T\delta\gamma_\omega^\circ + M_t\delta\kappa_{sz})dz \tag{20}$$

where $N_z, M_x, M_y, M_\omega, V_x, V_y, T, M_t$ are axial force, bending moments in the x- and y-direction, warping moment (bimoment), shear force in the x- and y-direction, and torsional moments, respectively, defined by integrating over the cross-sectional area A as

$$N_z = \int_A \sigma_z ds dn \tag{21a}$$

$$M_y = \int_A \sigma_z(x + n\sin\theta)dsdn \tag{21b}$$

$$M_x = \int_A \sigma_z(y - n\cos\theta)dsdn \tag{21c}$$

$$M_\omega = \int_A \sigma_z(\omega - nq)dsdn \tag{21d}$$

$$V_x = \int_A (\sigma_{sz}\cos\theta + \sigma_{nz}\sin\theta)dsdn \tag{21e}$$

$$V_y = \int_A (\sigma_{sz}\sin\theta - \sigma_{nz}\cos\theta)dsdn \tag{21f}$$

$$T = \int_A \Big[\sigma_{sz}r - \sigma_{nz}q\Big]dsdn \tag{21g}$$

$$M_t = \int_A \sigma_{sz}ndsdn \tag{21h}$$

On the other hand, the variation of work done by external forces can be written as

$$\delta\mathcal{V} = -\int_v (p_z\delta w + p_n\delta u + p_s\delta v)dv \tag{22}$$

where p_z, p_n, p_s are forces acting in z, n and s direction. The above expression can be written with respect to the shell forces and displacements by using Eq.(8)

$$\delta\mathcal{V} = -\int_0^l \int_s (\bar{p}_z\delta\bar{w} + \bar{p}_n\delta\bar{u} + \bar{p}_s\delta\bar{v} + \bar{m}_z\bar{\psi}_z + \bar{m}_s\bar{\psi}_s)dsdz \tag{23}$$

where $\bar{p}_z, \bar{p}_s, \bar{m}_z, \bar{m}_s, \bar{p}_n$ are shell forces defined by

$$(\bar{p}_z, \bar{m}_z) = \int_n p_z(1, n)dn \tag{24a}$$

$$(\bar{p}_s, \bar{m}_s) = \int_n p_s(1, n)dn \tag{24b}$$

$$\bar{p}_n = \int_n p_n dn \tag{24c}$$

After substituting Eqs.(1) and (5) into Eq.(23), the variation of the work done by the external forces can be written with respect to the bar forces

$$\delta\mathcal{V} = -\int_0^l [\mathcal{P}_z\delta W + \mathcal{V}_x\delta U + \mathcal{M}_y\delta\Psi_y + \mathcal{V}_y\delta V + \mathcal{M}_x\delta\Psi_x + \mathcal{T}\delta\Phi + \mathcal{M}_\omega\delta\Psi_\omega]dz \tag{25}$$

where the bar forces are related to the shell forces as

$$\mathcal{P}_z = \int_s \bar{p}_z ds \tag{26a}$$

$$\mathcal{V}_y = \int_s (\bar{p}_s\sin\theta - \bar{p}_n\cos\theta)ds \tag{26b}$$

$$\mathcal{V}_x = \int_s (\bar{p}_s\cos\theta + \bar{p}_n\sin\theta)ds \tag{26c}$$

$$\mathcal{T} = \int_s (\bar{p}_s r - \bar{p}_n q + \bar{m}_s)ds \tag{26d}$$

$$\mathcal{M}_y = \int_s (\bar{m}_z \sin\theta + \bar{p}_z x) ds \tag{26e}$$

$$\mathcal{M}_x = \int_s (-\bar{m}_z \cos\theta + \bar{p}_z y) ds \tag{26f}$$

$$\mathcal{M}_\omega = \int_s (-\bar{m}_z q + \bar{p}_z \omega) ds \tag{26g}$$

Principle of total potential energy can be stated as

$$0 = \delta\Pi = \delta\mathcal{U} + \delta\mathcal{V} \tag{27}$$

Substituting Eqs.(20) and (25) into Eq.(27), the weak form of the present theory for thin-walled composite space beams is given by

$$\begin{aligned} 0 = & \int_0^l \Big\{ N_z \delta W' + M_y \delta\Psi_y' + M_x \delta\Psi_x' + M_\omega \delta\Psi_\omega' + V_x \delta(U' + \Psi_y) + V_y \delta(V' + \Psi_x) + T\delta(\Phi' + \Psi_\omega) + M_t \delta(\Phi' - \Psi_\omega) \\ & - \mathcal{P}_z \delta W - \mathcal{V}_x \delta U - \mathcal{M}_y \delta\Psi_y - \mathcal{V}_y \delta V - \mathcal{M}_x \delta\Psi_x - \mathcal{T}\delta\Phi - \mathcal{M}_\omega \delta\Psi_\omega \Big] dz \end{aligned} \tag{28}$$

IV. CONSTITUTIVE EQUATIONS

The constitutive equations of a k^{th} orthotropic lamina in the laminate co-ordinate system of section are given by

$$\begin{Bmatrix} \sigma_z \\ \sigma_{sz} \end{Bmatrix}^k = \begin{bmatrix} \bar{Q}_{11}^* & \bar{Q}_{16}^* \\ \bar{Q}_{16}^* & \bar{Q}_{66}^* \end{bmatrix}^k \begin{Bmatrix} \epsilon_z \\ \gamma_{sz} \end{Bmatrix} \tag{29}$$

where $\bar{Q}_{ij}^*$ are transformed reduced stiffnesses and can be calculated from the transformed stiffnesses based on the plane stress ($\sigma_s = 0$) and plane strain ($\epsilon_s = 0$) assumption. More detailed explanation can be found in Ref.[32]

The constitutive relation for out-of-plane stress and strain is given by

$$\sigma_{nz} = \bar{Q}_{55} \gamma_{nz} \tag{30}$$

The constitutive equations for bar forces and bar strains are obtained by using Eqs.(16), (21), (29) and (30)

$$\begin{Bmatrix} N_z \\ M_y \\ M_x \\ M_\omega \\ M_t \\ V_x \\ V_y \\ T \end{Bmatrix} = \begin{bmatrix} E_{11} & E_{12} & E_{13} & E_{14} & E_{15} & E_{16} & E_{17} & E_{18} \\ & E_{22} & E_{23} & E_{24} & E_{25} & E_{26} & E_{27} & E_{28} \\ & & E_{33} & E_{34} & E_{35} & E_{36} & E_{37} & E_{38} \\ & & & E_{44} & E_{45} & E_{46} & E_{47} & E_{48} \\ & & & & E_{55} & E_{56} & E_{57} & E_{58} \\ & & & & & E_{66} & E_{67} & E_{68} \\ & & & & & & E_{77} & E_{78} \\ \text{sym.} & & & & & & & E_{88} \end{bmatrix} \begin{Bmatrix} \epsilon_z^\circ \\ \kappa_y \\ \kappa_x \\ \kappa_\omega \\ \kappa_{sz} \\ \gamma_{xz}^\circ \\ \gamma_{yz}^\circ \\ \gamma_\omega^\circ \end{Bmatrix} \tag{31}$$

where E_{ij} are stiffnesses of thin-walled composite beams and given in Ref.[29].

V. GOVERNING EQUATIONS

The equilibrium equations of the present study can be obtained by integrating the derivatives of the varied quantities by parts and collecting the coefficients of $\delta W, \delta U, \delta V, \delta\Phi, \delta\Psi_y, \delta\Psi_x$ and $\delta\Psi_\omega$

$$N_z' + \mathcal{P}_z = 0 \tag{32a}$$

$$V_x' + \mathcal{V}_x = 0 \tag{32b}$$

$$V_y' + \mathcal{V}_y = 0 \tag{32c}$$

$$M_t' + T' + \mathcal{T} = 0 \tag{32d}$$

$$M_y' - V_x + \mathcal{M}_y = 0 \tag{32e}$$

$$M_x' - V_y + \mathcal{M}_x = 0 \tag{32f}$$

$$M_\omega' + M_t - T + \mathcal{M}_\omega = 0 \tag{32g}$$

The natural boundary conditions are of the form

$$\delta W : \quad W = \overline{W}_0 \quad \text{or} \quad N_z = \overline{N}_{z_0} \tag{33a}$$

$$\delta U : \quad U = \overline{U}_0 \quad \text{or} \quad V_x = \overline{V}_{x_0} \tag{33b}$$

$$\delta V : \quad V = \overline{V}_0 \quad \text{or} \quad V_y = \overline{V}_{y_0} \tag{33c}$$

$$\delta\Phi : \quad \Phi = \overline{\Phi}_0 \quad \text{or} \quad T + M_t = \overline{T}_0 + \overline{M}_{t_0} \tag{33d}$$

$$\delta\Psi_y : \quad \Psi_y = \overline{\Psi}_{y_0} \quad \text{or} \quad M_y = \overline{M}_{y_0} \tag{33e}$$

$$\delta\Psi_x : \quad \Psi_x = \overline{\Psi}_{x_0} \quad \text{or} \quad M_x = \overline{M}_{x_0} \tag{33f}$$

$$\delta\Psi_\omega : \quad \Psi_\omega = \overline{\Psi}_{\omega_0} \quad \text{or} \quad M_\omega = \overline{M}_{\omega_0} \tag{33g}$$

Eq.(33g) denotes the warping restraint boundary condition. When the warping of the cross section is restrained, $\Psi_\omega = 0$ and when the warping is not restrained, $M_\omega = 0$.

By substituting Eqs.(15) and (31) into Eq.(32), the explicit form of the governing equations can be expressed with respect to the laminate stiffnesses E_{ij} as

$$\begin{aligned} &E_{11}W'' + E_{16}U'' + E_{17}V'' + (E_{15}+E_{18})\Phi'' + E_{12}\Psi_y'' + E_{16}\Psi_y' + E_{13}\Psi_x'' \\ &+E_{17}\Psi_x' + E_{14}\Psi_\omega'' + (E_{18}-E_{15})\Psi_\omega' + \mathcal{P}_z = 0 \end{aligned} \tag{34a}$$

$$E_{16}W'' + E_{66}U'' + E_{67}V'' + (E_{56}+E_{68})\Phi'' + E_{26}\Psi_y'' + E_{66}\Psi_y' + E_{36}\Psi_x''$$
$$+E_{67}\Psi_x' + E_{46}\Psi_\omega'' + (E_{68}-E_{56})\Psi_\omega' + \mathcal{V}_x = 0 \tag{34b}$$

$$E_{17}W'' + E_{67}U'' + E_{77}V'' + (E_{57}+E_{78})\Phi'' + E_{27}\Psi_y'' + E_{67}\Psi_y' + E_{37}\Psi_x''$$
$$+E_{77}\Psi_x' + E_{47}\Psi_\omega'' + (E_{78}-E_{57})\Psi_\omega' + \mathcal{V}_y = 0 \tag{34c}$$

$$(E_{15}+E_{18})W'' + (E_{56}+E_{68})U'' + (E_{57}+E_{78})V'' + (E_{55}+2E_{58}+E_{88})\Phi''$$
$$+(E_{25}+E_{28})\Psi_y'' + (E_{56}+E_{68})\Psi_y' + (E_{35}+E_{38})\Psi_x'' + (E_{57}+E_{78})\Psi_x'$$
$$+(E_{45}+E_{48})\Psi_\omega'' + (E_{88}-E_{55})\Psi_\omega' + \mathcal{T} = 0 \tag{34d}$$

$$E_{12}W'' - E_{16}W' + E_{26}U'' - E_{66}U' + E_{27}V'' - E_{67}V' + (E_{25}+E_{28})\Phi''$$
$$-(E_{56}+E_{68})\Phi' + E_{22}\Psi_y'' - E_{66}\Psi_y + E_{23}\Psi_x'' + (E_{27}-E_{36})\Psi_x' - E_{67}\Psi_x$$
$$+E_{24}\Psi_\omega'' + (E_{28}-E_{25}-E_{46})\Psi_\omega' + (E_{56}-E_{68})\Psi_\omega + \mathcal{M}_y = 0 \tag{34e}$$

$$E_{13}W'' - E_{17}W' + E_{36}U'' - E_{67}U' + E_{37}V'' - E_{77}V' + (E_{35}+E_{38})\Phi''$$
$$-(E_{57}+E_{78})\Phi' + E_{23}\Psi_y'' + (E_{36}-E_{67})\Psi_y' - E_{67}\Psi_y + E_{33}\Psi_x'' - E_{77}\Psi_x$$
$$+E_{34}\Psi_\omega'' + (E_{38}-E_{35}-E_{47})\Psi_\omega' + (E_{57}-E_{78})\Psi_\omega + \mathcal{M}_x = 0 \tag{34f}$$

$$E_{14}W'' + (E_{15}-E_{18})W' + E_{46}U'' + (E_{56}-E_{68})U' + E_{47}V'' + (E_{57}-E_{78})V'$$
$$+(E_{45}+E_{48})\Phi'' + (E_{55}-E_{88})\Phi' + E_{24}\Psi_y'' + (E_{25}-E_{28}+E_{46})\Psi_y'$$
$$+(E_{56}-E_{68})\Psi_y + E_{34}\Psi_x'' + (E_{35}-E_{38}+E_{47})\Psi_x' + (E_{57}-E_{78})\Psi_x$$
$$+E_{44}\Psi_\omega'' - (E_{55}-2E_{58}+E_{88})\Psi_\omega + \mathcal{M}_\omega = 0 \tag{34g}$$

Eq.(34) is most general form of thin-walled composite space beams with arbitrary lay-ups under external loads. For general anisotropic materials, the dependent variables, U, V, W, Φ, Ψ_x, Ψ_y and Ψ_ω are fully-coupled implying that the beam undergoes a coupled behavior involving bending, extension, twisting, transverse shearing, and warping. If

all the coupling effects are neglected, Eq.(34) can be simplified to the uncoupled differential equations as

$$(EA)_{com}W'' + \mathcal{P}_z = 0 \tag{35a}$$

$$(GA_y)_{com}(U'' + \Psi_y') + \mathcal{V}_x = 0 \tag{35b}$$

$$(GA_x)_{com}(V'' + \Psi_x') + \mathcal{V}_y = 0 \tag{35c}$$

$$(GJ_1)_{com}\Phi'' - (GJ_2)_{com}\Psi_\omega' + \mathcal{T} = 0 \tag{35d}$$

$$(EI_y)_{com}\Psi_y'' - (GA_y)_{com}(U' + \Psi_y) + \mathcal{M}_y = 0 \tag{35e}$$

$$(EI_x)_{com}\Psi_x'' - (GA_x)_{com}(V' + \Psi_x) + \mathcal{M}_x = 0 \tag{35f}$$

$$(EI_\omega)_{com}\Psi_\omega'' + (GJ_2)_{com}\Phi' - (GJ_1)_{com}\Psi_\omega + \mathcal{M}_\omega = 0 \tag{35g}$$

From above equations, $(EA)_{com}$ represents axial rigidity; $(GA_x)_{com}$, $(GA_y)_{com}$ represent shear rigidities with respect to x- and y-axis; $(EI_x)_{com}$ and $(EI_y)_{com}$ represent flexural rigidities with respect to x- and y-axis; $(EI_\omega)_{com}$ represents warping rigidity; and $(GJ_1)_{com}$, $(GJ_2)_{com}$ represent torsional rigidities of thin-walled composite beams, respectively, written as

$$(EA)_{com} = E_{11} \tag{36a}$$

$$(EI_y)_{com} = E_{22} \tag{36b}$$

$$(EI_x)_{com} = E_{33} \tag{36c}$$

$$(EI_\omega)_{com} = E_{44} \tag{36d}$$

$$(GA_y)_{com} = E_{66} \tag{36e}$$

$$(GA_x)_{com} = E_{77} \tag{36f}$$

$$(GJ_1)_{com} = E_{55} + E_{88} \tag{36g}$$

$$(GJ_2)_{com} = E_{55} - E_{88} \tag{36h}$$

VI. FINITE ELEMENT FORMULATION

The present theory for thin-walled composite space beams described in the previous section was implemented via a one-dimensional displacement-based finite element method. The generalized displacements are expressed over each element as a linear combination of the one-dimensional Lagrange interpolation function ψ_j associated with node j

and the nodal values

$$W = \sum_{j=1}^{n} w_j \psi_j \tag{37a}$$

$$U = \sum_{j=1}^{n} u_j \psi_j \tag{37b}$$

$$V = \sum_{j=1}^{n} v_j \psi_j \tag{37c}$$

$$\Phi = \sum_{j=1}^{n} \phi_j \psi_j \tag{37d}$$

$$\Psi_y = \sum_{j=1}^{n} \psi_{yj} \psi_j \tag{37e}$$

$$\Psi_x = \sum_{j=1}^{n} \psi_{xj} \psi_j \tag{37f}$$

$$\Psi_\omega = \sum_{j=1}^{n} \psi_{\omega j} \psi_j \tag{37g}$$

Substituting these expressions into the weak statement in Eq.(28), the finite element model of a typical element in the local coordinate can be expressed as

$$\begin{bmatrix} K_{11} & K_{12} & K_{13} & K_{14} & K_{15} & K_{16} & K_{17} \\ & K_{22} & K_{23} & K_{24} & K_{25} & K_{26} & K_{27} \\ & & K_{33} & K_{34} & K_{35} & K_{36} & K_{37} \\ & & & K_{44} & K_{45} & K_{46} & K_{47} \\ & & & & K_{55} & K_{56} & K_{57} \\ & & & & & K_{66} & K_{67} \\ \text{sym.} & & & & & & K_{77} \end{bmatrix} \begin{Bmatrix} w \\ u \\ v \\ \phi \\ \psi_y \\ \psi_x \\ \psi_\omega \end{Bmatrix} = \begin{Bmatrix} f_1 \\ f_2 \\ f_3 \\ f_4 \\ f_5 \\ f_6 \\ f_7 \end{Bmatrix} \tag{38}$$

or

$$[\overline{K}_e]\{\overline{\Delta}\}_e = \{\overline{f}_e\} \tag{39}$$

More detailed explanation explicit forms of the element stiffness matrix $[\overline{K}_e]$ and the element force vector $\{\overline{f}_e\}$ can be found in Ref.[29].

In order to transform element stiffness matrix in the local coordinate to those in the global coordinate, the trans-

formation matrix $[R]$ is needed as follows

$$\left\{\begin{array}{c} x \\ y \\ z \end{array}\right\} = \left[\begin{array}{ccc} \cos(x,X) & \cos(x,Y) & \cos(x,Z) \\ \cos(y,X) & \cos(y,Y) & \cos(y,Z) \\ \cos(z,X) & \cos(z,Y) & \cos(z,Z) \end{array}\right] \left\{\begin{array}{c} X \\ Y \\ Z \end{array}\right\} = [R] \left\{\begin{array}{c} X \\ Y \\ Z \end{array}\right\} \tag{40}$$

where $\cos(x, Z)$ indicates the direction cosine between the x axis in the local coordinate and the Z axis in the global coordinate.

Assuming that the bimoment is a scalar quantity, the element stiffness matrix and the element force vector in the global coordinate can be easily obtained through transformation

$$[K_e] = [T]^T[\overline{K}_e][T] \tag{41a}$$

$$\{f_e\} = [T]^T\{\overline{f}_e\} \tag{41b}$$

where $[T]$ is the 14×14 transformation matrix and given in Ref.[33]

$$[T] = \left[\begin{array}{cccccccc} [R] & & & & & & & \\ & [R] & & & 0 & & & \\ & & 1 & & & & & \\ & & & [R] & & & & \\ & & & & [R] & & & \\ \text{sym.} & & & & & & & 1 \end{array}\right] \tag{42}$$

Assemblage the element matrices for the entire structure leads to the structural stiffness equation for thin-walled composite space frames as

$$[K]\{\Delta\} = \{f\} \tag{43}$$

where $\{\Delta\}$ and $\{f\}$ are the unknown nodal displacements and the nodal force vectors, respectively in global coordinate.

VII. NUMERICAL EXAMPLES

For verification purpose, a simple three-dimensional orthogonal rigid space frame consisting of three members with geometry and cross-sectional dimensions as shown in Fig. 2, is analyzed. **Beam 1 is oriented along the X-axis, Beam 2 along the Z-axis and Beam 3 along the Y-axis, respectively. A transverse force in the Y-Z plane, along Y-axis $\mathrm{F_y} = 500$N is applied at the center of Beam 2**. In addition, the ends of three members

are restrained against warping at their common junction. The analyzes are usually based on plane stress conditions ($\sigma_s = 0$), unless specified otherwise. The following material properties are used

$$E_1 = 181.0\text{GPa}\,, E_2 = 10.3\text{GPa}\,, G_{12} = G_{13} = G_{23} = 7.17\text{GPa}\,, \nu_{12} = 0.28 \tag{44}$$

The definition of Bank and Cofie [23] called "Composite Structural Identification Pattern" (CSIP) is used again in this study. For the I-beam consisting of three panels, the top flange, web and bottom flange, the CSIP matrix has the following form

$$\text{CSIP} = \begin{bmatrix} \text{Stacking sequence of top flange} \\ \text{Stacking sequence of web} \\ \text{Stacking sequence of bottom flange} \end{bmatrix} \tag{45}$$

The same geometry and CSIP is used for all three members. The CSIPs for the composite-material I-beam frame members in this example are as follows

$$\text{CSIP}_1 = \begin{bmatrix} [+30^\circ]_{16} \\ [\pm 30^\circ]_{4s} \\ [+30^\circ]_{16} \end{bmatrix}, \quad \text{CSIP}_2 = \begin{bmatrix} [+30^\circ]_{16} \\ [\pm 30^\circ]_{4s} \\ [-30^\circ]_{16} \end{bmatrix} \tag{46}$$

The results of two stacking sequences CSIP_1 and CSIP_2 are plotted together to enable comparison between behaviors of each member. The angle of twist and displacements along the length of the Beam 2 and Beam 1 are shown in Figs. 3-6. By using both plane stress ($\sigma_s = 0$) and plane strain ($\epsilon_s = 0$) assumptions, the vertical displacement distribution along Beam 2 for CSIP_1 and angle of twist distribution along Beam 1 for CSIP_1 and CSIP_2 are illustrated in Figs. 5 and 6. A comparison of the results from present analysis with the solution in Ref.[23] shows a good agreement. It can be seen that the proposed model can capture all responses coming from material anisotropy with previous results. The difference between two solutions probably stems from assumptions of using equivalent one-dimensional mechanical properties for the estimation of the critical region of Bank and Cofie in Refs.[22-24].

In order to investigate the coupling, the same configuration with the previous example except the laminate stacking sequence is considered. The fiber angle is rotated in the web and flanges. The only difference between the CSIPs is in the orientation of the fiber angle in the bottom flange.

$$\text{CSIP}_{1\theta} = \begin{bmatrix} [+\theta^\circ]_{16} \\ [\pm \theta^\circ]_{4s} \\ [+\theta^\circ]_{16} \end{bmatrix}, \quad \text{CSIP}_{2\theta} = \begin{bmatrix} [+\theta^\circ]_{16} \\ [\pm \theta^\circ]_{4s} \\ [-\theta^\circ]_{16} \end{bmatrix} \tag{47}$$

For above lay-ups, the coupling stiffnesses E_{16}, E_{38} for $\text{CSIP}_{1\theta}$ and E_{18}, E_{36} for $\text{CSIP}_{2\theta}$, respectively, do not vanish while all the other coupling stiffnesses become zero. Especially, E_{36} and E_{38} become no more negligibly small as given in Table I. Due mainly to the applied load on Beam 2 causing a torsional moment in Beam 1 rather than anisotropic coupling, the angle of twist along Beam 1 of two lay-ups nearly coincides each other in Fig. 7. As expected, the angle of twist at junction is minimum at $\theta = 0^\circ$ and reaches maximum value at $\theta = 90^\circ$. It is from Figs. 8 and 9 that highlight the influence of the coupling effects on the torsional displacement along Beam 2 and Beam 3. This response of these members with two stacking sequences is very different. For lay-up $\text{CSIP}_{2\theta}$, no coupling induced twist effect takes place in Beam 2 and Beam 3, whereas for $\text{CSIP}_{1\theta}$, the angle of twist is clearly seen. It can be explained by the existence of coupling stiffness E_{38} in $\text{CSIP}_{1\theta}$. As fiber angle changes, the torsional displacement can vanish for some specific points along the Beam 2 implying that the angle of twist can be suppressed with carefully tailored stacking sequence. It should be noted that this response can not be observed when the coupling effects are ignored for instance at fiber angles $\theta = 0^\circ$ and 90°. For lay-up $\text{CSIP}_{2\theta}$, the lateral displacement in Beam 2 and Beam 3 are seen in Figs. 10 and 11 because coupling stiffness E_{36} induces flexure response. There is no such displacement shown in these members for all the fiber angles of lay-up $\text{CSIP}_{1\theta}$. It is implicated that the structure under transverse load not only causes vertical and torsional displacement as would be observed, but also causes additional response due solely to coupling effects. Since stacking sequence of $\text{CSIP}_{2\theta}$ is unsymmetric between the flanges, the lateral displacement along Beam 3 does not vanish for all fiber angles even for $\theta = 90^\circ$ in Fig. 11. The coupling effects becomes maximum about $\theta = 40^\circ$, thus, the largest lateral displacements of Beam 2 and Beam 3 occur around this value. At this fiber angle, the maximum negative value of lateral displacement in Beam 2 is about 250% of the positive one. Finally, the variation of vertical displacement distribution along Beam 2 with respect to fiber angle change for $\text{CSIP}_{1\theta}$ is plotted in Fig. 12. This deflection composes of three contribution of flexural, shearing and coupling effects. These effects decrease significantly with the increasing of fiber angle, and thus, the vertical displacement at the mid-span becomes larger for higher fiber angles and reaches maximum value at $\theta = 90^\circ$.

VIII. CONCLUDING REMARKS

A general analytical model is developed to study the flexural-torsional behavior of thin-walled composite space frames with arbitrary lay-ups under external loads. This model is capable of predicting accurately all flexural-torsional responses for various configuration including boundary conditions and laminate orientation. A one-dimensional 14 degree-of-freedom space beam model which includes the effects of shear deformation, warping and accounts for all

coupling coming from the material anisotropy is developed. The present analytical model is found to be appropriate and efficient in analyzing flexural-torsional problem of thin-walled composite space frames.

Acknowledgments

The support of the research reported here by Seoul R&BD Program through Grant GR070033 and by Korea Ministry of Construction and Transportation through Grant 2006-C106A1030001-06A050300220 is gratefully acknowledged. The authors also would like to thank Professor Lawrence C. Bank for his help.

References

[1] Vlasov VZ. Thin-walled elastic beams. 2nd Edition. Jerusalem, Israel: Israel Program for Scientific Translation; 1961.

[2] Gjelsvik A. The theory of thin-walled bars. New York: John Wiley and Sons Inc.; 1981.

[3] Volovoi VV, Hodges DH, Berdichevsky VL and Sutyrin V. Asymptotic theory for static behavior of elastic anisotropic I-beams. Int J Solids Struct 1999;36(7):1017-1043.

[4] Volovoi VV and Hodges DH. Theory of anisotropic thin-walled beams. J Appl Mech 2000;67(3):453-459.

[5] Yu W, Hodges DH, Volovoi VV and Fuchs ED. A generalized Vlasov theory for composite beams. Thin-Walled Struct 2005;43(9):1493-1511.

[6] Bauld, NR and Tzeng, LS. A Vlasov theory for fiber-reinforced beams with thin-walled open cross section. Int J Solids Struct 1984;20(3):277-297.

[7] Chandra R and Chopra I. Experimental and theoretical analysis of composite I beams with elastic couplings. AIAA J 1991;29(12):2197-2206.

[8] Kollar LP and Springer GS. Mechanics of composite structure. Cambridge University Press, 2003.

[9] Librescu L and Song 0. Thin-walled Composite Beams. Springer, 2006.

[10] Salim HA and Davalos JF. Torsion of Open and Closed Thin-Walled Laminated Composite Sections. J Compos Mater 2005;39(6):497-524.

[11] Pluzsik A and Kollar LP. Torsion of closed section, orthotropic, thin-walled beams. Int J Solids Struct 2006; 43(17):5307-5336.

[12] Kim MY, Kim NI and Shin DK. Exact solutions for thin-walled open-section composite beams with arbitrary lamination subjected to torsional moment. Thin-Walled Struct 2006; 44(6):638-654.

[13] Shin DK, Kim NI and Kim MY. Exact stiffness matrix of mono-symmetric composite I-beams with arbitrary lamination. Compos Struct 2007; 79(4):467-480.

[14] Piovan MT and Cortinez VH. Mechanics of shear deformable thin-walled beams made of composite materials. Thin-Walled Struct 2007;45(1):37-62.

[15] Back SY and Will KM. Shear-flexible thin-walled element for composite I-beams. Eng Struct 2008;30(5):1447-1458.

[16] Sheikh AH, Thomsen OT. An efficient beam element for the analysis of laminated composite beams of thin-walled open and closed cross sections. Compos Sci Technol 2008; 68(10-11):2273-2281.

[17] Noor AK, Peters JM and Min BJ. Mixed finite element models for free vibrations of thin-walled beams. Finite Elem Anal Des 1989; 5(4):291-305.

[18] Noor AK, Carden HD and Peters JM. Free vibrations of thin-walled semicircular graphite-epoxy composite frames. Finite Elem Anal Des 1991;9(1):33-63.

[19] Collins JS and Johnson ER. Static and Dynamic Response of Graphite-Epoxy Curved Frames. J Compos Mater 1992; 26(6):792-803.

[20] Bank LC and Cofie E. A modified beam theory for bending and twisting of open-section composite beams- Numerical verification. Compos Struct 1992; 21(1):29-39.

[21] Cofie E. Finite element analysis of the torsional behavior of thin-walled members using a warping superelement. In: Proc. AIAA 34th SDM Conference 1993:292-299.

[22] Cofie E. Analysis of thin-walled isotropic and anisotropic composite structures by the direct stiffness method. Ph.D thesis, The Catholic University of America, Washington DC, United States of America, 1993.

[23] Bank LC and Cofie E. A hybrid force/stiffness matrix method for the analysis of thin-walled composite frames. Compos Struct 1994; 28(4):391-404.

[24] Cofie E and Bank LC. Analysis of thin-walled anisotropic frames by the direct stiffness method. Int J Solids Struct 1995; 32(2):235-249.

[25] Ning H, Vaidya U, Janowski G and Husman G. Design, manufacture and analysis of a thermoplastic composite frame structure for mass transit. Compos Struct 2007; 80(1):105-116.

[26] Minghini F, Tullini N and Laudiero F. Buckling analysis of FRP pultruded frames using locking-free finite elements. Thin-Walled Struct 2008; 46(3):223-241.

[27] Minghini F, Tullini N and Laudiero F. Vibration analysis with second-order effects of pultruded FRP frames using locking-free elements. Thin-Walled Struct 2009; 47(2):136-150.

[28] Minghini F, Tullini N and Laudiero F. Elastic buckling analysis of pultruded FRP portal frames having semi-rigid connections. Eng Struct 2009; 31(2):292-299.

[29] Lee J. Flexural analysis of thin-walled composite beams using shear-deformable beam theory. Compos Struct 2005;70(2):212-222.

[30] Vo TP and Lee J. Flexural-torsional behavior of thin-walled composite box beams using shear-deformable beam theory.

Eng Struct 2008;30(7):1958-1968.

[31] Vo TP. Linear and nonlinear finite element analysis of thin-walled composite structures. Ph.D thesis, Sejong University, Seoul, South Korea, 2009.

[32] Jones RM. Mechanics of composite materials. New York: Hemisphere Publishing Corp.; 1975.

[33] Kim SB. Spatial stability and free vibration analysis of shear deformable thin-walled space frames and circular arches. Ph.D thesis, Seoul National University, Seoul, South Korea, 1995.

CAPTION OF TABLE

Table I: Ratio of coupling stiffnesses with respect to the flexural and shearing stiffness.

CAPTION OF FIGURES

Figure 1: Definition of coordinates in thin-walled open sections.

Figure 2: Geometry and cross-sectional dimensions of a thin-walled composite space frame.

Figure 3: Angle of twist distribution along Beam 2 for lay-ups CSIP_1 and CSIP_2.

Figure 4: Lateral displacement distribution along Beam 2 for lay-ups CSIP_1 and CSIP_2.

Figure 5: Vertical displacement distribution along Beam 2 for lay-up CSIP_1.

Figure 6: Angle of twist distribution along Beam 1 for lay-ups CSIP_1 and CSIP_2.

Figure 7: Variation of the angle of twist distribution along Beam 1 with respect to fiber angle change in the flanges and web for lay-ups $\text{CSIP}_{1\theta}$ and $\text{CSIP}_{2\theta}$.

Figure 8: Variation of the angle of twist distribution along Beam 2 with respect to fiber angle change in the flanges and web for lay-up $\text{CSIP}_{1\theta}$.

Figure 9: Variation of the angle of twist distribution along Beam 3 with respect to fiber angle change in the flanges and web for lay-up $\text{CSIP}_{1\theta}$.

Figure 10: Variation of the lateral displacement distribution along Beam 2 with respect to fiber angle change in the flanges and web for lay-up $\text{CSIP}_{2\theta}$.

Figure 11: Variation of the lateral displacement distribution along Beam 3 with respect to fiber angle change in the flanges and web for lay-up $\text{CSIP}_{2\theta}$.

Figure 12: Variation of the vertical displacement distribution along Beam 2 with respect to fiber angle change in the flanges and web for lay-up $\text{CSIP}_{1\theta}$.

TABLE I Ratio of coupling stiffnesses with respect to the flexural and shearing stiffness.

Fiber	$CSIP_{1\theta}$		$CSIP_{2\theta}$	
angle	E_{38}/E_{33}	E_{38}/E_{66}	E_{36}/E_{33}	E_{36}/E_{66}
0	0.0000	0.0000	0.0001	0.0000
15	-0.1360	-0.0004	9.0670	0.0267
30	-0.3493	-0.0003	23.2860	0.0231
45	-0.5762	-0.0002	38.4137	0.0150
60	-0.7399	-0.0001	49.3255	0.0091
75	-0.4938	-0.0001	32.9212	0.0045
90	0.0000	0.0000	3.8316	0.0000

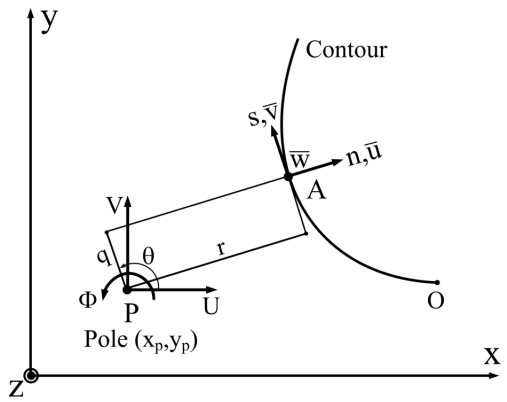

FIG. 1 Definition of coordinates in thin-walled open sections.

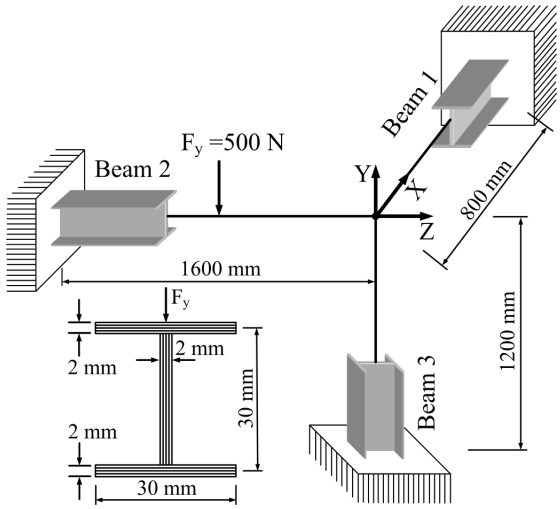

FIG. 2 Geometry and cross-sectional dimensions of a thin-walled composite space frame.

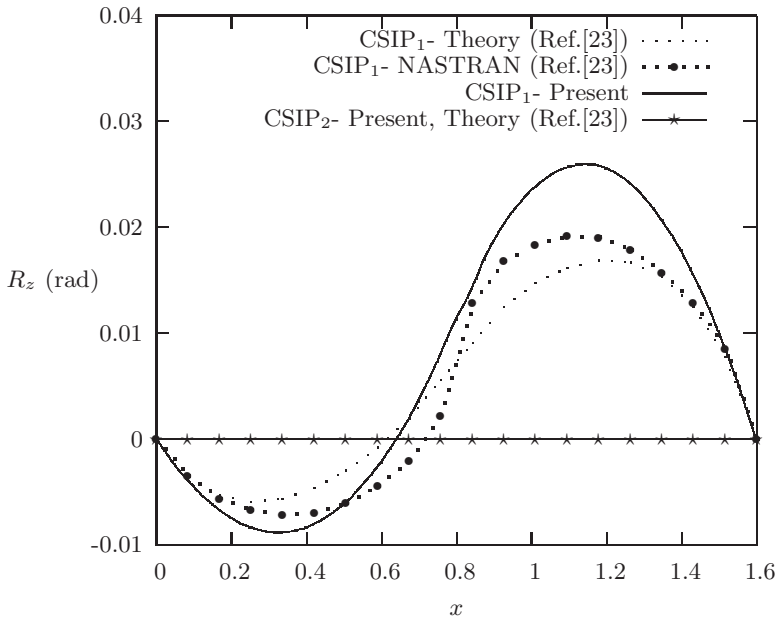

FIG. 3 Angle of twist distribution along Beam 2 for lay-ups CSIP$_1$ and CSIP$_2$.

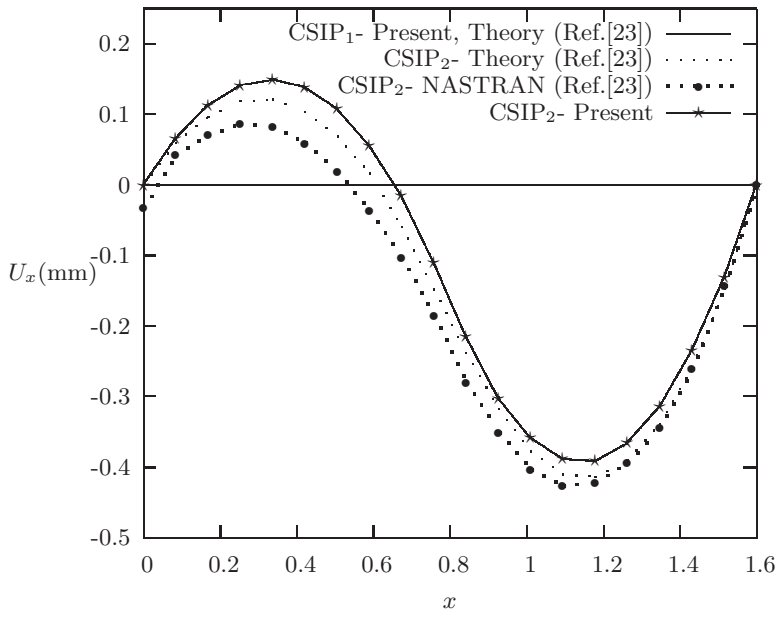

FIG. 4 Lateral displacement distribution along Beam 2 for lay-ups $CSIP_1$ and $CSIP_2$.

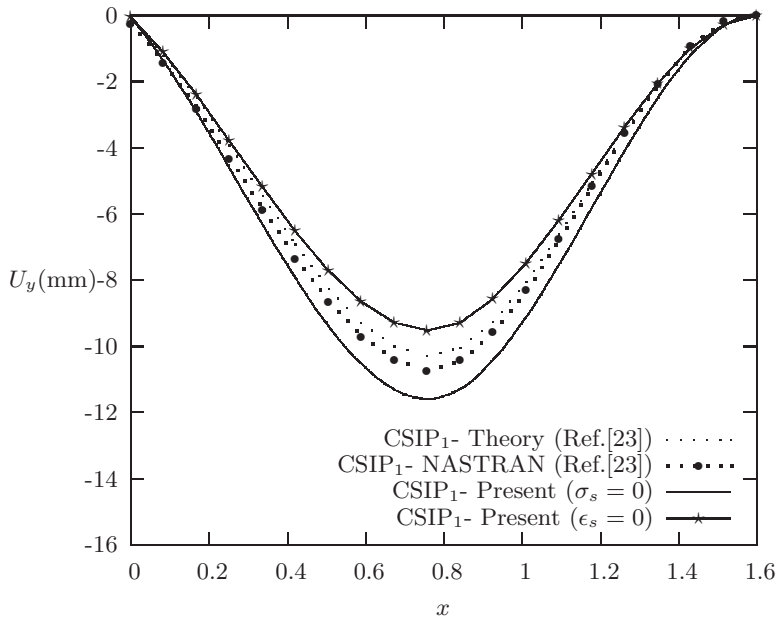

FIG. 5 Vertical displacement distribution along Beam 2 for lay-up CSIP$_1$.

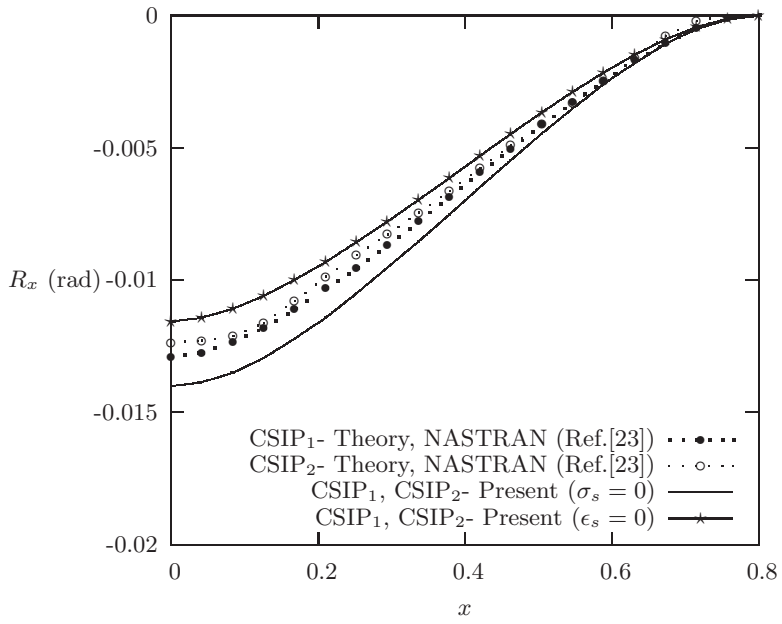

FIG. 6 Angle of twist distribution along Beam 1 for lay-ups CSIP$_1$ and CSIP$_2$.

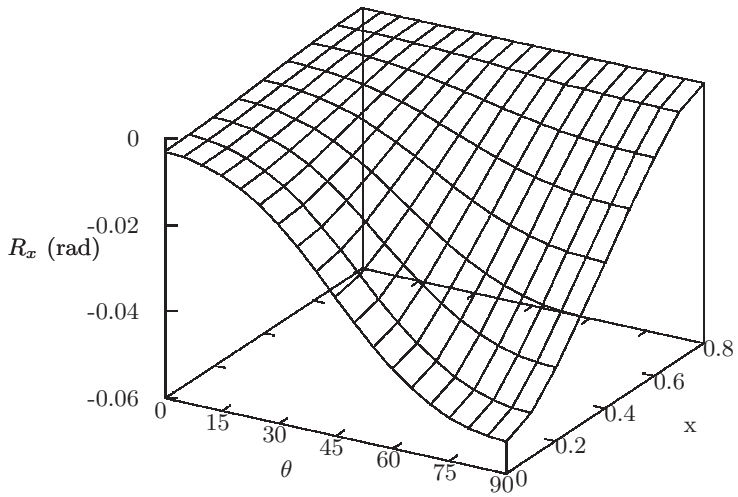

FIG. 7 Variation of the angle of twist distribution along Beam 1 with respect to fiber angle change in the flanges and web for lay-ups $\mathrm{CSIP}_{1\theta}$ and $\mathrm{CSIP}_{2\theta}$.

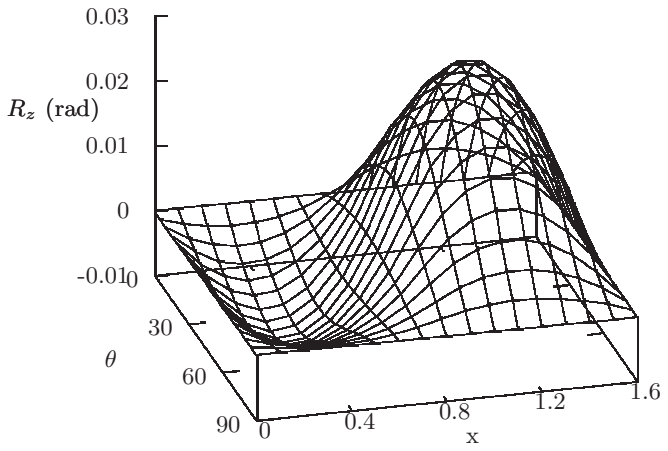

FIG. 8 Variation of the angle of twist distribution along Beam 2 with respect to fiber angle change in the flanges and web for lay-up $\text{CSIP}_{1\theta}$.

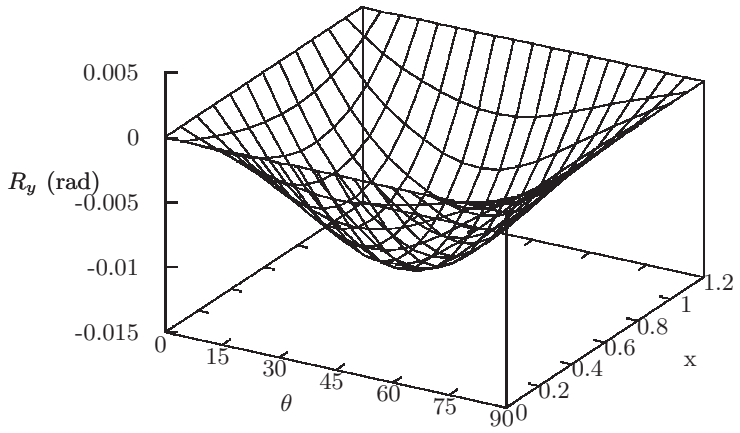

FIG. 9 Variation of the angle of twist distribution along Beam 3 with respect to fiber angle change in the flanges and web for lay-up $\text{CSIP}_{1\theta}$.

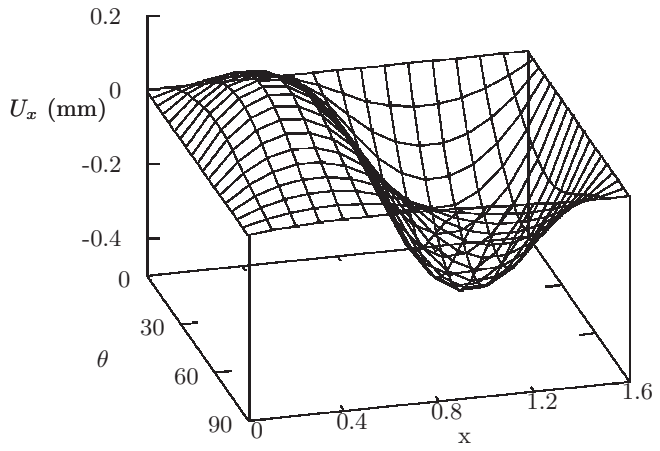

FIG. 10 Variation of the lateral displacement distribution along Beam 2 with respect to fiber angle change in the flanges and web for lay-up $\mathrm{CSIP}_{2\theta}$.

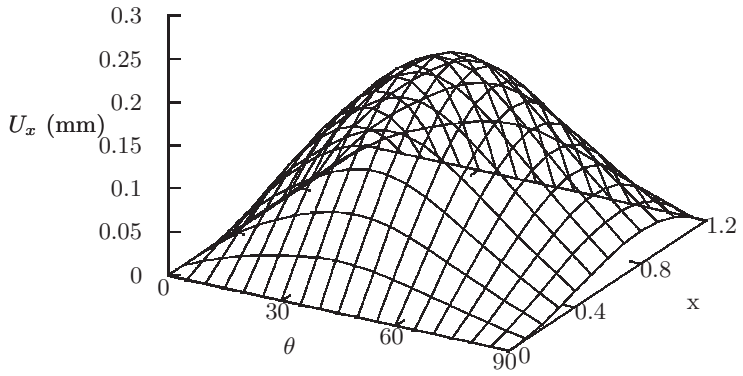

FIG. 11 Variation of the lateral displacement distribution along Beam 3 with respect to fiber angle change in the flanges and web for lay-up $\mathrm{CSIP}_{2\theta}$.

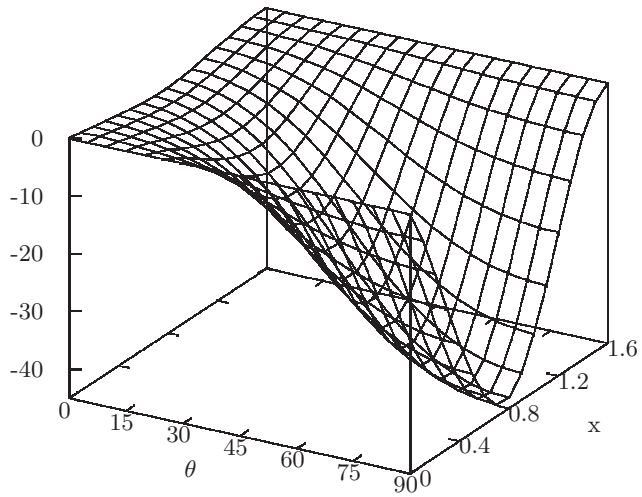

FIG. 12 Variation of the vertical displacement distribution along Beam 2 with respect to fiber angle change in the flanges and web for lay-up $\mathrm{CSIP}_{1\theta}$.